A centrifuge-based method for identifying novel genetic traits that affect root-substrate adhesion in *Arabidopsis thaliana*

Bethany M Eldridge[1,*], Emily R Larson[1,*], Laura Weldon[1,a], Kevin M Smyth[1], Annabelle N Sellin[1], Isaac V Chenchiah[2], Tanniemola B Liverpool[2] and Claire S Grierson[1,#]

[1]School of Biological Sciences, University of Bristol, Bristol Life Sciences Building, 24 Tyndall Avenue, Bristol, BS8 1TQ, UK

[2]School of Mathematics, University of Bristol, Fry Building, Woodland Road, Bristol BS8 1UG, UK

[a] Current address: Wildfowl and Wetlands Trust (WWT), Slimbridge, Gloucester, GL2 7BT, UK

[*]Authors contributed equally to this work.

[#]Corresponding author: Claire Grierson

lacsg@bristol.ac.uk

ORCID:

BME: ORCID: 0000-0002-6598-3701

ERL: ORCID: 0000-0002-5498-8152

LW: ORCID: 0000-0002-0761-4414

KMS: ORCID: 0000-0003-0105-8557

IVC: ORCID: 0000-0002-8618-620X

TBL: ORCID: 0000-0003-4376-5604

CSG: ORCID: 0000-0002-4000-0975

Keywords: Arabidopsis, Centrifuge assay, Forward genetics, Root exudates, Root hairs, Root-substrate adhesion, Survival analysis, Vesicle trafficking and Secretion

Running title: Centrifuge-based assay measures root adhesion

ABSTRACT

The physical presence of roots and the compounds they release affect the cohesion between roots and their environment. However, the plant traits that are important for these interactions are unknown and most methods that quantify the contributions of these traits are time-intensive and require specialist equipment and complex substrates. Our lab developed an inexpensive, high-throughput phenotyping assay that quantifies root-substrate adhesion in *Arabidopsis thaliana*. We now report that this method has high sensitivity and versatility for identifying different types of traits affecting root-substrate adhesion including root hair morphology, vesicle trafficking pathways and root exudate composition. We describe a practical protocol for conducting this assay and introduce its use in a forward genetic screen to identify novel genes affecting root-substrate interactions. This assay is a powerful tool for identifying and quantifying genetic contributions to cohesion between roots and their environment.

INTRODUCTION

Plants secrete compounds that help them adapt to their environment, sense and interact with other organisms, and improve water and nutrient uptake (reviewed in Bais et al., 2006; Sasse et al., 2018; Vives-Peris et al., 2020). These compounds (exudates) can vary in composition based on plant species, developmental stage, and environment (Naveed et al., 2017). Recent studies have shown that some compounds have bioadhesive properties that stick plants and soils together and aggregate soil particles, modifying the microenvironment around plant roots (Galloway et al., 2018). However, understanding how plant biology and physiology contribute to plant-soil interactions can be confounded by multiple factors like other organisms living in the soil that also secrete organic metabolites that can contribute to soil cohesion. Soil composition might affect plant exudate composition and vice versa. Also, plant root morphology including root architecture and the presence of root hairs can alter root-soil interactions (Bailey et al., 2002; Burylo et al., 2012; De Baets et al., 2007; Ghestem et al., 2014; Stokes et al., 2009). This complexity has made it difficult to characterise the relevant plant physiology.

We developed a high-throughput assay that identifies and quantifies the contribution of root hair cells to root-substrate cohesion in a less variable environment than the natural rhizosphere (De Baets et al., 2020). The assay uses a centrifuge to apply force to *Arabidopsis thaliana* seedlings grown on the surface of a sterile medium and measures the force required to detach seedlings from that surface, using a Cox proportional hazards regression (Prentice and Kalbfleisch, 2003) to quantify the adherence of candidate Arabidopsis lines relative to

wild-type plants at increasing centrifugal force. Previous use of this assay assessed whether presence or absence of root hairs affected adhesion to the agar (De Baets *et al.,* 2020) but did not address subtle aspects of root hair biology. We now wanted to test whether this assay is sensitive enough to identify other types of traits involved in root-substrate adhesion. To validate this extended use of the assay, we asked if it could detect the adhesive effects in (1) mutants with altered root hair shape; (2) vesicle trafficking mutants with no known root hair morphological defects; (3) exudate compositional mutants with no known root hair phenotypes; and (4) a forward genetic screen of a mutant population to identify novel genes that affect root-substrate adhesion.

Here, we show that this method has the sensitivity to identify how differences in root hair morphology and biological functions that do not present a visible root hair phenotype contribute to substrate cohesion. Using the genetic and molecular tools available in Arabidopsis and working in a sterile environment allows hypotheses about plant specific factors of root-substrate interactions to be tested. While plant-soil cohesion is a complex and dynamic interaction, our assay provides a way to efficiently probe root cellular functions that might be masked by confounding variables in a soil-based study system. Results from this assay provide a platform for more comprehensive studies of plant morphology and physiology that affect root-substrate cohesion.

MATERIALS AND METHODS

Materials and Equipment

1. 20% [v/v] bleach solution
2. Sterile distilled water
3. Seed for candidate Arabidopsis lines
4. Half strength Murashige and Skoog basal medium
5. 1% [w/v] sucrose
6. 1% [w/v] agar
7. Laminar air hood
8. 90-mm triple vented Petri Plates
9. Parafilm
10. Growth room
11. Swing-out bucket centrifuge
12. Laboratory safety razor blade
13. Analytical balance

103

104 **Plant Material and Growth Conditions**

105 Candidate and wild-type lines of the Columbia-0 (Col-0) ecotype of *Arabidopsis*
106 *thaliana* single-gene mutants were obtained from the Nottingham Arabidopsis Stock Centre
107 (NASC; Nottingham, UK) or were stocks maintained in the lab (**Table 1**). Homozygous lines
108 were used in all experiments.

109 For all experiments, seeds were surface sterilised for 15 min in 20% [v/v] bleach and
110 sterile water solution, followed by five washes in sterile water. All sterilised seeds were
111 stratified in the dark at 4°C for 24-48 h in Eppendorf microtubes containing sterile water. All
112 plants were reared in a growth room at 21-22°C with a continuous photoperiod (light intensity
113 = 120-145 µmol m^{-2} s^{-1}) at 60% humidity.

114 Half strength Murashige and Skoog basal medium was supplemented with 1% [w/v]
115 sucrose pH adjusted to 5.7, solidified with 1% [w/v] agar. A 30 ml volume of sterilized media
116 (at ~45 – 50°C) was pipetted into 90-mm triple vented Petri plates and left to set for ~30 min
117 in a laminar air hood. Sterilized seeds were sown onto Petri plates containing the sterile
118 medium and sealed with Parafilm. Plates were then placed in stacks of five at ~80° from the
119 horizontal (lid side up) to encourage vertical growth along the gel surface. Plates were
120 incubated in the growth chamber for 5-6 days before centrifugation. Plants for genomic DNA
121 extractions were grown in compost (three parts Levington F3 compost and one-part J Arthur
122 Bowers horticultural silver sand).

123

124 **Centrifuge Assay Set-Up**

125 To measure the adhesion of Arabidopsis seedling roots using a centrifuge, seedling
126 roots must not penetrate the gel or touch each other, as both events could interfere with seedling
127 detachment during centrifugation. Therefore, ten seeds were sown 1-cm apart on each plate in
128 two parallel rows (**Figure 1Ai**). The plates were then grown for 5-6 days (**Figure 1Aii**) and
129 seedlings that were touching each other, had grown into the gel, or not uniform in size were
130 omitted from the assay. The seedlings were then numbered so that plate positional effects could
131 be included as a potential covariate in the final analysis (**Figure 1Bi**). Plates were inverted and
132 placed into a swing-out bucket centrifuge (Beckman Allegra X-30R Centrifuge) that held four
133 plates at a time and subjected to increments of increasing centrifugal force at 720, 1018, 1247,
134 1440 and 1611 RPM for one minute each (**Figure 1Bii**). The proportion of seedlings that
135 detached from the gel surface was recorded between each centrifugal speed; a detachment
136 event was recorded when a seedling had partially or fully peeled away from the gel (**Figure**

137 **1Biii**). If the gel shattered during the assay, seedlings that had not detached from the gel were
138 not recorded and seedlings that remained adhered to the gel after the maximum centrifugal
139 speed were censored in the analysis. During method optimisation we encountered some
140 common methodological challenges for which we provide troubleshooting options in **Table**
141 **S1**.
142
143 **Calculating Seedling Detachment Force**
144 To calculate the centrifugal force acting on a seedling, the aerial tissue mass for each
145 seedling was separated from the root by making an incision at the hypocotyl-root junction using
146 a laboratory safety razor blade and immediately measured using an analytical balance (**Figure**
147 **1Ci, ii**). The aerial tissue weight of each seedling was measured because a plant with heavier
148 aerial tissue experiences more force than a lighter one subjected to the same centrifugal speed.
149 Centrifugal force, Fc (mN) acting on a seedling was calculated as previously reported in De
150 Baets et al. (2020). Aerial tissue weight (kg), the angular velocity (ω) and the distance between
151 the seedling and the axis of rotation on the centrifuge (radius = 0.07m) were used to give the
152 following equation:
153
154 $Fc = mass \times radius \times \omega^2$ (Equation 1)
155
156 **Identification of *abcg43-1* Mutant T-DNA Insert**
157 Genomic DNA was extracted from a pool of vegetative tissue taken from ten three-
158 week old plants using an adapted protocol (Healey et al., 2014) for Illumina Next-Generation
159 two x paired-end sequencing conducted at the Bristol Genomics Facility (University of Bristol,
160 UK). The Illumina TruSeq Nano LT gDNA kit (Illumina Inc) was used to generate a genomic
161 DNA sequencing library following the manufacturer's protocol. The final library was diluted
162 to a loading concentration of 1.4 pM for cluster generation and 2 x 150 bp paired-end
163 sequencing on the Illumina NextSeq500 system (Illumina Inc) alongside a 5% PhiX spike-in
164 control library. Read summary statistics were generated using the RTA 2.4.6 Primary Analysis
165 Software (Illumina Inc). The read summaries were analysed in the Sequencing Analysis
166 Viewer (Illumina Inc). Filtered paired reads were subject to paired-end alignment using the
167 Bowtie2 2.3.4.2 aligner (Langmead and Salzberg, 2012). A bespoke reference genome was
168 produced that combined the TAIR10 Arabidopsis genome (Lamesch et al., 2012) and the
169 pROK2 vector sequence (Baulcombe et al., 1986). Alignments were viewed in the Integrative
170 Genomics Viewer IGV 2.3 (Robinson et al., 2011).

171 For Sanger sequencing, DNA was extracted from a pool of vegetative tissue taken from
172 two-week-old plants using a modified Edwards prep (Edwards et al., 1991). High fidelity PCR
173 was conducted on the *abcg43-1* line using the Q5 High-Fidelity 2X Master Mix (NEB). PCR
174 products were purified and extracted from a 1% agarose gel using the QIAquick Gel Extraction
175 Kit (QIAGEN), following the manufacturer's instructions. Purified PCR product plus the
176 *abcg43-1* forward, reverse or border genotyping primer (**Table S2**) was used for Sanger
177 sequencing (using the Mix2Seq overnight sequencing kit, Eurofins Genomics).
178 Chromatograms and FASTA files were obtained from Eurofin Genomics and following manual
179 low-quality end trimming, the final sequences were aligned to the pROK2 vector sequence and
180 *ABCG43* gene sequence using the MUSCLE alignment tool (Madeira et al., 2019).
181
182 **Genotyping**
183 To genotype the *abcg43* mutant alleles, genomic DNA was extracted from the vegetative tissue
184 of two-week-old plants using a modified Edwards prep (Edwards et al., 1991). T-DNA border
185 and gene-specific primers were used in PCR analyses to confirm the genotype (**Table S2**).
186
187 **Morphological Root Trait Analyses**
188 Five-day-old Arabidopsis seedlings were imaged with a Leica MZ FLIII microscope
189 (Leica) with dark-field lighting. Root hair length and density were measured using microscope
190 images of five-day-old Arabidopsis seedlings and Fiji version 1.0 (Schindelin et al., 2012) and
191 the Bio-Formats Importer plugin. At least two experimental repeats were conducted; in each
192 experiment, we imaged eight to ten individual plants from each line and measured at least 30
193 root hairs per plant.
194
195 **Statistical Analyses**
196 All statistical analyses were conducted using RStudio, version 1.1453 (R Core Team,
197 2014) and all graphs were generated using the R package ggplot2 (Wickham, 2016).
198 A Cox proportional hazards (PH) regression model was used to statistically test for
199 differences between the detachment of experimental seedlings relative to the wild-type control
200 (Col-0) at increasing force (**Figure 1Ciii)**. Cox PH regression models were conducted using
201 the coxph function within the survival package in R and in all cases, the assumption of
202 proportionality was satisfied. Comparisons of different candidate lines relative to the wild type
203 line were analysed *a priori*; therefore, a series of contrasts were set up using the R function
204 contr.treatment rather than using post-hoc testing methods. Seedling position and individual

205 plate number were incorporated as covariates to account for any heterogeneity; when these
206 covariates had no significant effect, they were removed from the model. We censored seedlings
207 that remained attached to the gel after the maximum centrifugal speed because we did not
208 determine the speed these seedlings would have detached from the gel. For each Cox PH
209 regression model run, we report the P value of the Wald Statistic (*z*-score) and the hazard ratio
210 with the upper and lower bound confidence intervals. An alpha level of 0.01 was used. The
211 root-gel detachment of at least 70 plants from each line was assessed within a single
212 experiment.
213 Univariate analyses were conducted using the lm function in R to test for differences in
214 the mean root hair density or mean root hair length (of eight to ten individual plants from each
215 line) between candidate lines relative to wild type. In all cases, the assumptions of normality
216 and homoscedasticity were satisfied. Because comparisons of different mutant lines relative to
217 the wild type line were *a priori*, a series of contrasts were conducted using the contr.treatment
218 function in R. To prevent type I errors from multiple testing, we applied the Bonferroni method
219 and adjusted the alpha level to 0.025 (0.05/2).
220
221 **RESULTS**
222 **Root Hair Morphological Effects on Root-Substrate Adhesion**
223 We screened mutant lines with known root hair morphology defects to ask if the
224 centrifuge assay could determine if root hair shape affects root-substrate adhesion. The mostly
225 bald mutant *csld3*, which encodes the CESA-like 3D protein (Favery et al., 2001; Wang et al.,
226 2001; Yang et al., 2020) was included as a root hairless example. For lines that produce short
227 or malformed root hairs, we included the *gdi1-2* Rho GTPase GDP dissociation inhibitor
228 mutant, *rol1-2* rhamnose biosynthesis 1 mutant allele, *can of worms 1* (*cow1-3*)
229 phosphatidylinositol transferase protein mutant, and *lrx1-4* leucine rich extensin 1 mutant
230 (Baumberger et al., 2001; Böhme et al., 2004; Carol et al., 2005; Diet et al., 2006; Grierson et
231 al., 1997). The *rol1-2* and *gdi1-2* mutants have short root hairs and the root hairs on *gdi1-2*
232 plants can also branch (Diet et al., 2006; Kang et al., 2017; Parker et al., 2000; Ringli et al.,
233 2008). *cow1-3* plants have short, wide root hairs that can branch, whilst *lrx1-4* plants can
234 develop root hairs that abort, swell, branch, or collapse in a growth condition-dependent
235 manner (Baumberger et al., 2001; Böhme et al., 2004; Grierson et al., 1997; Parker et al., 2000).
236 Assay results for ectopic root hairs and long root hairs were reported previously (De Baets et
237 al., 2020). Under our growth conditions, we confirmed the reported phenotypes for each mutant
238 line (**Figure 2A**). Wild type was used as the baseline group for all centrifuge experiments, with

239 a hazard ratio of one. Therefore, a candidate line with a higher risk of detachment from the gel
240 than wild type will have a hazard ratio above one, while lines with a lower risk of detachment
241 than wild type will have a hazard ratio below one.
242 Consistent with previous results (De Baets et al., 2020), bald (*csld3*) seedlings detached
243 at lower centrifugal forces relative to wild-type seedlings, with 4.6 times the risk of detachment
244 than wild-type plants (z = 8.644, P<0.001, HR = 4.636, 95% CI = 3.274 – 6.564; **Figure 2B**).
245 Mutants with deformed root hair phenotypes including *gdi1-2, rol1-2, cow1-3* and *lrx1-4* had
246 risks of detachment that were 2.5, 4, 3.8 and 3.9 times that of wild-type plants, respectively
247 (*gdi1-2* – z = 5.199, P<0.001, HR = 2.459, 95% CI = 1.752 – 3.452; *rol1-2* – z = 7.927, P<0.001,
248 HR = 4.036, 95% CI = 2.858 – 5.698; *cow1-3* – z = 7.350, P<0.001, HR = 3.790, 95% CI =
249 2.657 – 5.407; *lrx1-4* – z = 8.049, P<0.001, HR = 3.926, 95% CI = 2.814 – 5.478; **Figure 2B-**
250 **D**). These results indicated that the centrifuge assay can quantify the effects of root hair shape
251 on root-substrate cohesion. Many of the root hair mutants tested are associated with changes
252 in root hair cell wall composition, suggesting that alterations in secreted compounds could
253 affect root-substrate interactions in addition to any physical or surface area-related factors that
254 are specific to root hairs.
255
256 **Vesicle Trafficking Mutations Affect Root-Substrate Adhesion**
257 We hypothesized that Arabidopsis mutants with defective vesicle trafficking pathways
258 might alter cell wall and apoplast characteristics that contribute to root-substrate interactions
259 and adhesion. We chose the secretory Soluble NSF (N-ethylmaleimide sensitive fusion protein)
260 Attachment proteins (SNAP) REceptor (SNARE) mutants *syp121* and *syp122-1*, and the
261 endocytic mutants, *chc1-2* and *chc2-3* as candidates for our assay. SYP121 is the primary
262 secretory SNARE found on the plasma membrane (Assaad et al., 2004; Geelen et al., 2002)
263 and has characterized aboveground phenotypes, including small rosettes and stomatal mobility
264 defects (Eisenach et al., 2012; Larson et al., 2017); however, the mutant does not have a
265 reported root hair phenotype. Although the related SNARE SYP122 is thought to share partial
266 functionality with SYP121, the *syp122-1* mutant does not share these phenotypes with *syp121*
267 and a recent proteomic analysis reported differences in their vesicle cargoes, which could
268 contribute to their functional independence (Waghmare et al., 2018). The *chc1-2* and *chc2-3*
269 mutants are defective in the heavy chain subunits of the clathrin coat complex, which is
270 required for vesicle traffic at the plasma membrane (Kitakura et al., 2011; Mbengue et al.,
271 2016). Endo- and exocytic rates are impaired in both mutants (Larson et al., 2017), but no root
272 hair phenotypes have been reported. For the centrifuge assay, it was important to select mutants

273 that do not have root hair phenotypes given the effect root hair morphology has on root-gel
274 adhesion. Therefore, we evaluated the root hairs of these vesicle trafficking mutants and found
275 that the root hairs of these lines did not significantly differ from wild-type plants (**Figure 3A**).
276 Overall, the risk of detachment for *syp121, syp122-1, chc1-2* and *chc2-3* plants was 3.6,
277 3.3, 4.5 and 3.9 times that of wild type, respectively (*syp121* – z = 7.702, P<0.001, HR = 3.593,
278 95% CI = 2.595 – 4975; *syp122-1* – z = 7.199, P<0.001, HR = 3.270, 95% CI = 2.369 – 4.515;
279 *chc1-2* – z = 8.238, P<0.001, HR = 4.482, 95% CI = 3.137 – 6.405; *chc2-3* – z = 7.653, P<0.001,
280 HR = 3.941, 95% CI = 2.774 – 5.599; **Figure 3B,C**). Given that all the mutants detached from
281 the gel at lower centrifugal forces than wild-type seedlings, these results indicated that the
282 corresponding genes contribute to root-substrate adhesion and that the centrifuge assay can be
283 used to probe for intracellular molecular machinery that affect root-substrate interactions.
284
285 **Exudate Composition Changes Root Detachment Rates**
286 Over 20% of plant assimilated carbon is released as root exudates (Huang et al., 2016).
287 These are complex mixtures of diverse molecular forms that can modify the external
288 environment in response to abiotic and biotic stimuli. Some exudate components contribute to
289 soil adhesion (Akhtar et al., 2018; Galloway et al., 2018). Root epidermal and hair cells secrete
290 compounds that contribute to root exudate profiles that can be plant species specific (Naveed
291 et al., 2017). Because mutants in both root hair development and vesicle trafficking pathways
292 showed root-substrate adhesion phenotypes (**Figure 2 and 3**), we asked if the centrifuge assay
293 could identify effects of exudate composition on root-substrate adhesion. We selected
294 Arabidopsis mutants reported to have altered exudate composition compared to wild type,
295 including *pft1-3*, *jin1-9*, and *pdr2* (Badri et al., 2009; Berger et al., 1996; Carvalhais et al.,
296 2015; Kidd et al., 2009). *PFT1* (*MED25*) encodes the MEDIATOR25 subunit of the Mediator
297 nuclear protein, and *JIN1* (*MYC2*) encodes a basic helix-loop-helix leucine zipper transcription
298 factor; both proteins are involved in the jasmonate signalling pathway (Kidd et al., 2009;
299 Lorenzo et al., 2004). *pft1-3* and *jin1-9* mutants are reported to have altered root exudate
300 composition, including lower amounts of the amino acids asparagine, ornithine and tryptophan
301 than wild-type plants (Carvalhais et al., 2015). *PDR2* (*ABCG30*) encodes a pleiotropic drug
302 resistance (PDR) full-length ABC transporter that is involved in ABA transport and the
303 exudation of secondary metabolites (Badri et al., 2008; Kang et al., 2015). We did not observe
304 root hair growth phenotypes in these mutant lines compared to wild type (**Figure 4A**).
305 Compared to wild-type seedlings, *pdr2* seedlings resisted detachment, with 0.38 times
306 the risk of detaching from the gel (z = -5.765, P<0.001, HR = 0.379, 95% CI = 0.273 – 0.528;

307 **Figure 4B**). Conversely, *pft1-3* seedlings had an increased risk of detachment 1.7 times that of
308 wild-type plants (z = 3.315, P<0.001, HR = 1.698, 95% CI = 1.242 – 2.323), and there was no
309 difference in gel adhesion between *jin1-9* and wild-type plants (z = 0.737, P>0.05, HR = 1.124,
310 95% CI = 0.824 – 1.537; **Figure 4B**). These results show that exudate composition can alter
311 root-substrate interactions, although this may not be the case for all exudate compositional
312 changes, or the effects of the exudate composition of the *jin1-9* mutant lay outside the
313 sensitivity range of the assay. Since these mutant lines did not have root hair phenotypes, our
314 results suggest that changes in exudate composition can alter root adhesive properties without
315 affecting plant root hair morphology, further indicating the power of the centrifuge assay as an
316 efficient mutant screening method.
317
318 **Centrifuge Assay as a Method for Forward Genetic Screening**
319 Having demonstrated that our centrifugation technique can identify different types of
320 traits that affect root-substrate adhesion, we used it in a forward genetic screen to find novel
321 genes involved in root-substrate adhesion. To conduct this screen, the root-gel adhesion
322 properties of individual plants from a pooled SALK T-DNA insertion mutant collection were
323 analysed (Alonso et al., 2003). Individual plants that detached at the lowest centrifugal speed
324 or remained attached to the gel after being spun at the highest centrifugal speed were recovered
325 from the screen and self-fertilized to obtain progeny and identify the putative mutations. The
326 centrifuge assay was used to rescreen the progeny (using a sample size of ≥ 70 n) to confirm
327 whether candidate lines had significantly increased or decreased root-gel adhesion relative to
328 wild-type plants. From this screen, we identified a line with significantly enhanced root-gel
329 adhesion and conducted genomic Next-Generation sequencing followed by Sanger sequencing
330 of T-DNA flanking PCR products to confirm a T-DNA insertion in the ABC transporter gene,
331 *ABCG43,* whose function is unknown. We named this T-DNA insertion line *abcg43-1* and
332 identified two additional mutant alleles, *abcg43-2* (SALK_201207c) and *abcg43-3*
333 (SALKseq_30713) (**Figure 5A**).
334 We analysed the root-gel adhesion of the homozygous insertional *ABCG43* mutant
335 alleles and found *abcg43-1*, *abcg43-2* and *abcg43-3* had detachment risks 0.25, 0.35 and 0.2
336 times that of wild-type plants, respectively (*abcg43-1* – z = -7.823, P<0.001, HR = 0.245, 95%
337 CI = 0.172 – 0.348; *abcg43-2* – z = -6.049, P<0.001, HR = 0.355, 95% CI = 0.253 – 0.496;
338 *abcg43-3* – z = -7.179, P<0.001, HR = 0.203 – 0.403; **Figure 5B, C**). Collectively, these results
339 suggested that disruption of *ABCG43* expression affects root-gel adhesion. These results also
340 illustrate the use of the centrifuge assay as a powerful screening method for identifying novel

genes involved in root-substrate adhesion, as well as a tool for evaluating the effects of known gene function on root-substrate interactions. Experiments are now being conducted to identify mutant trait(s) in these lines and understand how *ABCG43* affects root-substrate adhesion.

DISCUSSION

To date, most published methods that quantify the contribution of particular traits to plant-soil interactions are time-intensive and expensive (Bailey et al., 2002; De Baets and Poesen, 2010; De Baets et al., 2020; Toukura et al., 2006). In contrast, our assay can produce data within a week, is available to any laboratory with access to a bench top centrifuge and does not require speciality consumables. This method is a high-throughput and quantitative way to test the effects of root morphology and cell function on root-substrate adhesion and to screen for new biological and molecular factors that can alter plant-substrate interactions. Using a defined model system like Arabidopsis and sterile medium conditions permits the identification of plant-specific characteristics that can then be probed in other substrate- or soil-based conditions.

Using the Centrifuge Assay to Investigate the Role of Root Hairs in Root-Substrate Interactions

Results presented in this paper show that the centrifuge assay can quantify effects of root hair morphology on plant-substrate adhesion. Previous work has shown that the presence of root hairs can significantly enhance root-substrate adhesion compared to the absence of root hairs (Choi and Cho, 2019; De Baets et al., 2020; Haling et al., 2013). We now show that our centrifuge assay can distinguish the adherence strength of seedlings with altered root hair shapes and sizes (**Figure 2**) and can quantify the contribution these morphological traits make to plant-substrate interactions. Some mutants with defective root hairs have mutations in cell wall biosynthesis and modification proteins, so it is possible that altered root-substrate interface compromises adhesion in these mutants, not just root hair shape. Using our method to rapidly phenotype mutants with root hair growth defects could direct additional experiments to characterize biochemical and morphological properties of genes of interest. Indeed, current evidence for the importance of root hairs for the deposition of complex polysaccharides with soil-binding properties (Galloway et al., 2020) supports the need for assays such as ours to expedite the identification of genes and mechanisms that improve soil-remediation, top soil maintenance, and erosion tolerance of at-risk land.

375 **Identifying New Genes Involved in Root-Substrate Adhesion**

376 Mutations in cellular functions that do not alter root hair growth but do affect substrate
377 adhesion can also be investigated using this assay. Vesicle trafficking pathways are required
378 for cell wall deposition and maintenance (De Caroli et al., 2011; Larson et al., 2014; Rodriguez-
379 Furlán et al., 2016); therefore, we hypothesized that mutants in vesicle trafficking pathways,
380 particularly those at the plasma membrane, could affect root-substrate adhesion. Similarly, the
381 composition and deposition of plant exudates help plants modify and optimize their growth
382 conditions (Carvalhais et al., 2015; Naveed et al., 2017), suggesting that modification to plant
383 exudate composition could affect root-substrate interactions. Consistent with these hypotheses,
384 mutants with vesicle trafficking defects and altered exudate composition had root-substrate
385 adhesion properties that differed from wild type, indicating that this method can identify
386 aspects of plant cell biology important for root-substrate interactions that do not affect root or
387 root hair morphology (**Figures 3 and 4**). Our results further indicate that while root hairs
388 provide significant adhesive and cohesive support both on solid gel and soil media (De Baets
389 et al., 2020), there are additional cellular factors contributing to plant-substrate interactions that
390 are not directly observable without the use of expensive reagents, development of time-
391 intensive transgenic lines, and microscopy equipment. Our centrifuge assay provides an
392 affordable and quick alternative to these current methodologies.

393 The compounds and interactions that contribute to root-substrate adhesion are complex,
394 and the direct and indirect factors that participate in these interactions still remain to be
395 characterised in detail. Many root cell wall or secreted compounds might directly affect
396 adhesive characteristics of the root surface, such as arabinogalactan proteins involved in the
397 adhesion of English ivy (Huang et al., 2016). Other complex polysaccharides have also been
398 shown to enhance soil binding in both Arabidopsis and cereal root systems (Galloway et al.,
399 2018, 2020). Indeed, mutants in genes associated with the production of these compounds
400 would be potentially excellent candidates for the application of this assay, which would
401 quantify the contribution these compounds make to root-substrate adhesion.

402 We cannot expect all exudate components to present adhesive phenotypes because not
403 all will affect root-substrate adhesion, and some will affect adhesion in a way that is not
404 detected by this assay. For example, the *jin1-9* mutant tested in our exudate cohort was not
405 significantly more or less adhesive compared to wild-type roots (**Figure 4**) despite its altered
406 exudate composition (Anderson et al., 2004). Some exudate components will play no role in
407 adhesion, while others may require additional co-factors present in soil or non-sterile media to
408 participate in root-substrate interactions. Although these are examples of the limitations of the

assay, this assay does allow for the identification of direct contributions that plants make to root-substrate cohesion and its robust statistical power and high-throughput aspects will significantly improve genetic screening timelines and enhance large-scale experimental design.

Forward genetic screening relies on distinctive phenotypes that distinguish differences within large, genetically diverse populations. High throughput, creative assaying techniques to identify phenotypes within morphologically similar populations, such as thermal imaging (Plessis et al., 2011) and confocal imaging platforms (Drakakaki et al., 2011; Robert et al., 2008) require specific equipment that not all laboratories have at their disposal. In contrast, the centrifuge assay can be used as a screen to identify new genes affecting plant-substrate interactions without specialist equipment, making it an accessible option for research groups that may not otherwise be able to efficiently conduct genetic screens. Moreover, the centrifuge assay does not require morphological or conditional differences for candidate selection. As an example, we report the identification in a forward genetics screen of a mutant population in which *abcg43* mutant seedlings were identified and shown to be more adhesive to gel than wild type (**Figure 5**). The function of ABCG43 in Arabidopsis is uncharacterised, indicating that this assay can identify novel candidate genes that have no previously known association with root morphological defects, adhesion or exudate composition for future study.

CONCLUSION

This assay has applications in plant cell biology and genetics to investigate how diverse gene activities, cell functions and root structure affect plant-soil adhesion, and identify the molecular pathways involved. Potential applications not tested in this report include the measurement of the effects environmental conditions have on plant-substrate adhesion and how other plant species or ecotypes respond to detachment forces. Given the recent discovery that root hair presence is important for Arabidopsis cohesion between roots and gel, and compost or soil (De Baets *et al.,* 2020), this assay can broadly contribute to plant and soil sciences through the identification of plant traits that increase root-substrate cohesion and potentially stabilise slopes or reduce soil erosion.

SUPPLEMENTARY INFORMATION

Table S1 Centrifuge assay troubleshooting

Table S2 Primers used in this study for genotyping *Arabidopsis thaliana* mutants

ACKNOWLEDGEMENTS

This work was supported by a Leverhulme Trust project grant RPG-2013-260 to CSG and TBL. BME was supported by a BBSRC SWBio PhD studentship (grant BB/M009122/1). We are thankful to Don Grierson FRS and Enrico Coen FRS who independently suggested the centrifuge assay concept, Timothy Quine for providing insightful guidance during method development, and Thomas Denbigh for providing technical advice. We are grateful to Jill Harrison, Victoria Spencer, Zoe Nemec Venza, Sophie Carpenter and Nicholas H Fair for their helpful comments during revision of the manuscript. This manuscript has been released as a pre-print at [http://doi.org/10.1101/2020.05.14.095448] (Eldridge et al., 2020).

AUTHOR CONTRIBUTIONS

CSG designed the initial project, conducted proof-of-concept pilot experiments, obtained funding, and recruited and advised the team. TBL and IC developed the theoretical parameters for the centrifugal assay and the bounds on the errors from other mechanical forces. BME and ERL planned and conducted all experiments apart from the initial genetic screen, which was carried out by LW and KMS. BME and ERL analysed all of the data presented herein. AS and BME optimised the centrifuge assay data collection and data analysis methods. BME and ERL wrote the initial manuscript. BME, ERL, and CSG edited the manuscript. All authors reviewed and approved the final manuscript.

REFERENCES

Akhtar, J., Galloway, A.F., Nikolopoulos, G., Field, K.J., and Knox, P. (2018). A quantitative method for the high throughput screening for the soil adhesion properties of plant and microbial polysaccharides and exudates. Plant Soil *428*, 57–65.

Alonso, J.M., Stepanova, A.N., Leisse, T.J., Kim, C.J., Chen, H., Shinn, P., Stevenson, D.K., Zimmerman, J., Barajas, P., Cheuk, R., et al. (2003). Genome-wide insertional mutagenesis of Arabidopsis thaliana. Science *301*, 653–657.

Anderson, J.P., Badruzsaufari, E., Schenk, P.M., Manners, J.M., Desmond, O.J., Ehlert, C., Maclean, D.J., Ebert, P.R., and Kazan, K. (2004). Antagonistic Interaction between Abscisic Acid and Jasmonate-Ethylene Signaling Pathways Modulates Defense Gene Expression and Disease Resistance in Arabidopsis. The Plant Cell *16*, 3460–3479.

Assaad, F.F., Qiu, J.-L., Youngs, H., Ehrhardt, D., Zimmerli, L., Kalde, M., Wanner, G., Peck, S.C., Edwards, H., Ramonell, K., et al. (2004). The PEN1 Syntaxin Defines a Novel Cellular Compartment upon Fungal Attack and Is Required for the Timely Assembly of Papillae. Mol. Biol. Cell *15*, 5118–5129.

477 Badri, D.V., Loyola-Vargas, V.M., Broeckling, C.D., De-la-Peña, C., Jasinski, M., Santelia,
478 D., Martinoia, E., Sumner, L.W., Banta, L.M., Stermitz, F., et al. (2008). Altered Profile of
479 Secondary Metabolites in the Root Exudates of Arabidopsis ATP-Binding Cassette
480 Transporter Mutants. Plant Physiology *146*, 762–771.

481 Badri, D.V., Quintana, N., El Kassis, E.G., Kim, H.K., Choi, Y.H., Sugiyama, A., Verpoorte,
482 R., Martinoia, E., Manter, D.K., and Vivanco, J.M. (2009). An ABC transporter mutation
483 alters root exudation of phytochemicals that provoke an overhaul of natural soil microbiota.
484 Plant Physiol. *151*, 2006–2017.

485 Bailey, P.H.J., Currey, J.D., and Fitter, A.H. (2002). The role of root system architecture and
486 root hairs in promoting anchorage against uprooting forces in Allium cepa and root mutants
487 of Arabidopsis thaliana. J. Exp. Bot. *53*, 333–340.

488 Bais, H.P., Weir, T.L., Perry, L.G., Gilroy, S., and Vivanco, J.M. (2006). The role of root
489 exudates in rhizosphere interactions with plants and other organisms. Annu Rev Plant Biol
490 *57*, 233–266.

491 Baulcombe, D.C., Saunders, G.R., Bevan, M.W., Mayo, M.A., and Harrison, B.D. (1986).
492 Expression of biologically active viral satellite RNA from the nuclear genome of transformed
493 plants. Nature *321*, 446–449.

494 Baumberger, N., Ringli, C., and Keller, B. (2001). The chimeric leucine-rich repeat/extensin
495 cell wall protein LRX1 is required for root hair morphogenesis in Arabidopsis thaliana.
496 Genes Dev. *15*, 1128–1139.

497 Berger, S., Bell, E., and Mullet, J.E. (1996). Two Methyl Jasmonate-Insensitive Mutants
498 Show Altered Expression of AtVsp in Response to Methyl Jasmonate and Wounding. Plant
499 Physiology *111*, 525–531.

500 Böhme, K., Li, Y., Charlot, F., Grierson, C., Marrocco, K., Okada, K., Laloue, M., and
501 Nogué, F. (2004). The Arabidopsis COW1 gene encodes a phosphatidylinositol transfer
502 protein essential for root hair tip growth. Plant J. *40*, 686–698.

503 Burylo, M., Rey, F., Mathys, N., and Dutoit, T. (2012). Plant root traits affecting the
504 resistance of soils to concentrated flow erosion. Earth Surface Processes and Landforms *37*,
505 1463–1470.

506 Carol, R.J., Takeda, S., Linstead, P., Durrant, M.C., Kakesova, H., Derbyshire, P., Drea, S.,
507 Zarsky, V., and Dolan, L. (2005). A RhoGDP dissociation inhibitor spatially regulates
508 growth in root hair cells. Nature *438*, 1013–1016.

509 Carvalhais, L.C., Dennis, P.G., Badri, D.V., Kidd, B.N., Vivanco, J.M., and Schenk, P.M.
510 (2015). Linking Jasmonic Acid Signaling, Root Exudates, and Rhizosphere Microbiomes.
511 Mol. Plant Microbe Interact. *28*, 1049–1058.

512 Choi, H.-S., and Cho, H.-T. (2019). Root hairs enhance Arabidopsis seedling survival upon
513 soil disruption. Scientific Reports *9*, 11181.

514 Collins, N.C., Thordal-Christensen, H., Lipka, V., Bau, S., Kombrink, E., Qiu, J.-L.,
515 Hückelhoven, R., Stein, M., Freialdenhoven, A., Somerville, S.C., et al. (2003). SNARE-
516 protein-mediated disease resistance at the plant cell wall. Nature *425*, 973–977.

517 De Baets, S., and Poesen, J. (2010). Empirical models for predicting the erosion-reducing
518 effects of plant roots during concentrated flow erosion. Geomorphology *118*, 425–432.

519 De Baets, S., Poesen, J., Knapen, A., and Galindo, P. (2007). Impact of root architecture on
520 the erosion-reducing potential of roots during concentrated flow. Earth Surface Processes and
521 Landforms *32*, 1323–1345.

522 De Baets, S., Denbigh, T.D., Smyth, K.M., Eldridge, B.M., Weldon, L.M., Higgins, B.W.,
523 Matyjaszkiewicz, A.W., Meersmans, J., Larson, E.R., Chenchiah, I.V., et al. (2020). Micro-
524 scale interactions between Arabidopsis root hairs and soil particles influence soil erosion.
525 Nature Comms Biol *3*, 1–11.

526 De Caroli, M., Lenucci, M.S., Di Sansebastiano, G.-P., Dalessandro, G., De Lorenzo, G., and
527 Piro, G. (2011). Dynamic protein trafficking to the cell wall. Plant Signal Behav *6*, 1012–
528 1015.

529 Diet, A., Link, B., Seifert, G.J., Schellenberg, B., Wagner, U., Pauly, M., Reiter, W.-D., and
530 Ringli, C. (2006). The Arabidopsis root hair cell wall formation mutant lrx1 is suppressed by
531 mutations in the RHM1 gene encoding a UDP-L-rhamnose synthase. Plant Cell *18*, 1630–
532 1641.

533 Drakakaki, G., Robert, S., Szatmari, A.-M., Brown, M.Q., Nagawa, S., Van Damme, D.,
534 Leonard, M., Yang, Z., Girke, T., Schmid, S.L., et al. (2011). Clusters of bioactive
535 compounds target dynamic endomembrane networks in vivo. Proceedings of the National
536 Academy of Sciences *108*, 17850–17855.

537 Edwards, K., Johnstone, C., and Thompson, C. (1991). A simple and rapid method for the
538 preparation of plant genomic DNA for PCR analysis. Nucleic Acids Res *19*, 1349.

539 Eisenach, C., Chen, Z.-H., Grefen, C., and Blatt, M.R. (2012). The trafficking protein
540 SYP121 of Arabidopsis connects programmed stomatal closure and K^+ channel activity with
541 vegetative growth. Plant J. *69*, 241–251.

542 Eldridge, B.M., Larson, E.R., Weldon, L., Smyth, K.M., Sellin, A.N., Chenchiah, I.V.,
543 Liverpool, T.B., and Grierson, C.S. (2020). A centrifuge-based method for identifying novel
544 genetic traits that affect root-substrate adhesion in Arabidopsis thaliana. BioRxiv
545 2020.05.14.095448.

546 Favery, B., Ryan, E., Foreman, J., Linstead, P., Boudonck, K., Steer, M., Shaw, P., and
547 Dolan, L. (2001). KOJAK encodes a cellulose synthase-like protein required for root hair cell
548 morphogenesis in Arabidopsis. Genes Dev. *15*, 79–89.

549 Galloway, A.F., Pedersen, M.J., Merry, B., Marcus, S.E., Blacker, J., Benning, L.G., Field,
550 K.J., and Knox, J.P. (2018). Xyloglucan is released by plants and promotes soil particle
551 aggregation. New Phytol. *217*, 1128–1136.

552 Galloway, A.F., Akhtar, J., Marcus, S.E., Fletcher, N., Field, K., and Knox, P. (2020). Cereal
553 root exudates contain highly structurally complex polysaccharides with soil-binding
554 properties. The Plant Journal *103*, 1666–1678.

555 Geelen, D., Leyman, B., Batoko, H., Di Sansebastiano, G.-P., Moore, I., Blatt, M.R., and Di
556 Sansabastiano, G.-P. (2002). The abscisic acid-related SNARE homolog NtSyr1 contributes

557 to secretion and growth: evidence from competition with its cytosolic domain. Plant Cell *14*,
558 387–406.

559 Ghestem, M., Cao, K., Ma, W., Rowe, N., Leclerc, R., Gadenne, C., and Stokes, A. (2014). A
560 framework for identifying plant species to be used as "ecological engineers" for fixing soil on
561 unstable slopes. PLoS ONE *9*, e95876.

562 Grierson, C.S., Roberts, K., Feldmann, K.A., and Dolan, L. (1997). The COW1 locus of
563 arabidopsis acts after RHD2, and in parallel with RHD3 and TIP1, to determine the shape,
564 rate of elongation, and number of root hairs produced from each site of hair formation. Plant
565 Physiol *115*, 981–990.

566 Haling, R.E., Brown, L.K., Bengough, A.G., Young, I.M., Hallett, P.D., White, P.J., and
567 George, T.S. (2013). Root hairs improve root penetration, root-soil contact, and phosphorus
568 acquisition in soils of different strength. J. Exp. Bot. *64*, 3711–3721.

569 Healey, A., Furtado, A., Cooper, T., and Henry, R.J. (2014). Protocol: a simple method for
570 extracting next-generation sequencing quality genomic DNA from recalcitrant plant species.
571 Plant Methods *10*, 21.

572 Huang, Y., Wang, Y., Tan, L., Sun, L., Petrosino, J., Cui, M.-Z., Hao, F., and Zhang, M.
573 (2016). Nanospherical arabinogalactan proteins are a key component of the high-strength
574 adhesive secreted by English ivy. Proc. Natl. Acad. Sci. U.S.A. *113*, E3193-3202.

575 Kang, E., Zheng, M., Zhang, Y., Yuan, M., Yalovsky, S., Zhu, L., and Fu, Y. (2017). The
576 Microtubule-Associated Protein MAP18 Affects ROP2 GTPase Activity during Root Hair
577 Growth1[OPEN]. Plant Physiol *174*, 202–222.

578 Kang, J., Yim, S., Choi, H., Kim, A., Lee, K.P., Lopez-Molina, L., Martinoia, E., and Lee, Y.
579 (2015). Abscisic acid transporters cooperate to control seed germination. Nat Commun *6*,
580 8113.

581 Kidd, B.N., Edgar, C.I., Kumar, K.K., Aitken, E.A., Schenk, P.M., Manners, J.M., and
582 Kazan, K. (2009). The mediator complex subunit PFT1 is a key regulator of jasmonate-
583 dependent defense in Arabidopsis. Plant Cell *21*, 2237–2252.

584 Kitakura, S., Vanneste, S., Robert, S., Löfke, C., Teichmann, T., Tanaka, H., and Friml, J.
585 (2011). Clathrin mediates endocytosis and polar distribution of PIN auxin transporters in
586 Arabidopsis. Plant Cell *23*, 1920–1931.

587 Lamesch, P., Berardini, T.Z., Li, D., Swarbreck, D., Wilks, C., Sasidharan, R., Muller, R.,
588 Dreher, K., Alexander, D.L., Garcia-Hernandez, M., et al. (2012). The Arabidopsis
589 Information Resource (TAIR): improved gene annotation and new tools. Nucleic Acids Res.
590 *40*, D1202-1210.

591 Langmead, B., and Salzberg, S.L. (2012). Fast gapped-read alignment with Bowtie 2. Nat
592 Methods *9*, 357–359.

593 Larson, E.R., Domozych, D.S., and Tierney, M.L. (2014). SNARE VTI13 plays a unique role
594 in endosomal trafficking pathways associated with the vacuole and is essential for cell wall
595 organization and root hair growth in arabidopsis. Ann. Bot. *114*, 1147–1159.

596 Larson, E.R., Van Zelm, E., Roux, C., Marion-Poll, A., and Blatt, M.R. (2017). Clathrin
597 Heavy Chain Subunits Coordinate Endo- and Exocytic Traffic and Affect Stomatal
598 Movement. Plant Physiol. *175*, 708–720.

599 Lorenzo, O., Chico, J.M., Sánchez-Serrano, J.J., and Solano, R. (2004). JASMONATE-
600 INSENSITIVE1 encodes a MYC transcription factor essential to discriminate between
601 different jasmonate-regulated defense responses in Arabidopsis. Plant Cell *16*, 1938–1950.

602 Madeira, F., Park, Y.M., Lee, J., Buso, N., Gur, T., Madhusoodanan, N., Basutkar, P., Tivey,
603 A.R.N., Potter, S.C., Finn, R.D., et al. (2019). The EMBL-EBI search and sequence analysis
604 tools APIs in 2019. Nucleic Acids Res *47*, W636–W641.

605 Mbengue, M., Bourdais, G., Gervasi, F., Beck, M., Zhou, J., Spallek, T., Bartels, S., Boller,
606 T., Ueda, T., Kuhn, H., et al. (2016). Clathrin-dependent endocytosis is required for
607 immunity mediated by pattern recognition receptor kinases. Proc Natl Acad Sci U S A *113*,
608 11034–11039.

609 Naveed, M., Brown, L.K., Raffan, A.C., George, T.S., Bengough, A.G., Roose, T., Sinclair,
610 I., Koebernick, N., Cooper, L., Hackett, C.A., et al. (2017). Plant exudates may stabilize or
611 weaken soil depending on species, origin and time. European Journal of Soil Science *68*,
612 806–816.

613 Parker, J.S., Cavell, A.C., Dolan, L., Roberts, K., and Grierson, C.S. (2000). Genetic
614 interactions during root hair morphogenesis in Arabidopsis. Plant Cell *12*, 1961–1974.

615 Plessis, A., Cournol, R., Effroy, D., Silva Pérez, V., Botran, L., Kraepiel, Y., Frey, A., Sotta,
616 B., Cornic, G., Leung, J., et al. (2011). New ABA-hypersensitive Arabidopsis mutants are
617 affected in loci mediating responses to water deficit and Dickeya dadantii infection. PLoS
618 ONE *6*, e20243.

619 Prentice, R.L., and Kalbfleisch, J.D. (2003). Mixed discrete and continuous Cox regression
620 model. Lifetime Data Anal *9*, 195–210.

621 R Core Team (2014). R: A language and environment for statistical computing (Vienna,
622 Austria: R Foundation for Statistical Computing).

623 Ringli, C., Bigler, L., Kuhn, B.M., Leiber, R.-M., Diet, A., Santelia, D., Frey, B., Pollmann,
624 S., and Klein, M. (2008). The Modified Flavonol Glycosylation Profile in the Arabidopsis
625 rol1 Mutants Results in Alterations in Plant Growth and Cell Shape Formation. The Plant
626 Cell *20*, 1470–1481.

627 Robert, S., Chary, S.N., Drakakaki, G., Li, S., Yang, Z., Raikhel, N.V., and Hicks, G.R.
628 (2008). Endosidin1 defines a compartment involved in endocytosis of the brassinosteroid
629 receptor BRI1 and the auxin transporters PIN2 and AUX1. PNAS *105*, 8464–8469.

630 Robinson, J.T., Thorvaldsdóttir, H., Winckler, W., Guttman, M., Lander, E.S., Getz, G., and
631 Mesirov, J.P. (2011). Integrative genomics viewer. Nat. Biotechnol. *29*, 24–26.

632 Rodriguez-Furlán, C., Salinas-Grenet, H., Sandoval, O., Recabarren, C., Arraño-Salinas, P.,
633 Soto-Alvear, S., Orellana, A., and Blanco-Herrera, F. (2016). The Root Hair Specific
634 SYP123 Regulates the Localization of Cell Wall Components and Contributes to
635 Rizhobacterial Priming of Induced Systemic Resistance. Front Plant Sci *7*, 1081.

636 Sasse, J., Martinoia, E., and Northen, T. (2018). Feed Your Friends: Do Plant Exudates Shape
637 the Root Microbiome? Trends Plant Sci. *23*, 25–41.

638 Schindelin, J., Arganda-Carreras, I., Frise, E., Kaynig, V., Longair, M., Pietzsch, T.,
639 Preibisch, S., Rueden, C., Saalfeld, S., Schmid, B., et al. (2012). Fiji: an open-source
640 platform for biological-image analysis. Nat. Methods *9*, 676–682.

641 Stokes, A., Atger, C., Bengough, A.G., Fourcard, T., and Sidle, R.C. (2009). Desirable plant
642 root traits for protecting natural and engineered slopes against landslides. Plant and Soil *324*,
643 1–30.

644 Toukura, Y., Devee, E., and Hongo, A. (2006). Uprooting and shearing resistances in the
645 seedlings of four weedy species. Weed Biology and Management *6*, 35–43.

646 Vives-Peris, V., de Ollas, C., Gómez-Cadenas, A., and Pérez-Clemente, R.M. (2020). Root
647 exudates: from plant to rhizosphere and beyond. Plant Cell Rep. *39*, 3–17.

648 Waghmare, S., Lileikyte, E., Karnik, R., Goodman, J.K., Blatt, M.R., and Jones, A.M.E.
649 (2018). SNAREs SYP121 and SYP122 Mediate the Secretion of Distinct Cargo Subsets.
650 Plant Physiology *178*, 1679–1688.

651 Wang, X., Cnops, G., Vanderhaeghen, R., De Block, S., Van Montagu, M., and Van
652 Lijsebettens, M. (2001). AtCSLD3, A Cellulose Synthase-Like Gene Important for Root Hair
653 Growth in Arabidopsis. Plant Physiol *126*, 575–586.

654 Wickham, H. (2016). ggplot2: Elegant Graphics for Data Analysis (Springer).

655 Yang, J., Bak, G., Burgin, T., Barnes, W.J., Mayes, H.B., Peña, M.J., Urbanowicz, B.R., and
656 Nielsen, E. (2020). Biochemical and Genetic Analysis Identify CSLD3 as a beta-1,4-Glucan
657 Synthase That Functions during Plant Cell Wall Synthesis. Plant Cell *32*, 1749–1767.

658

659

660 **TABLES**

661 **Table 1** *Arabidopsis thaliana* mutant lines used in this study.

Mutant type	***Mutant***	***AGI code[a]***	***Mutant line***	***Referenced in***
Root hair shape	*cow1-3*	At4g34580	SALK_002124	Böhme *et al.* (2004)
	csld3-1	At3g03050	CS899	Wang *et al.* (2001)
	lrx1-4	At1g12040	SALK_057038	Baumberger *et al.* (2001)
	rol1-2	At1g78570	CS16373	Diet *et al.* (2006)
	gdi1-2	At3g07880	SALK_035400	Kang *et al.* (2017)
Vesicle trafficking	*chc1-2*	At3g11130	SALK_103252	Kitakura *et al.* (2011)
	chc2-3	At3g08530	SALK_151638	Mbengue *et al.* (2016)
	syp121	At3g11820	-	Collins *et al.* (2003)
	syp122-1	At3g52400	SALK_008617	Assaad *et al.* (2004)
Root exudate composition	*jin1-9*	At1g32640	SALK_017005	Anderson *et al.* (2004)
	pdr2	At4g15230	SAIL_811_F08	Badri *et al.* (2008)
	pft1-3	At1g25540	SALK_059316	Kidd *et al.* (2009)
Unknown	*abcg43-1*	At4g15236	N75206[b]	This study
	abcg43-2	At4g15236	SALK_201207	This study
	abcg43-3	At4g15236	SALKseq_30713	This study

662

663

664 **FIGURE LEGENDS**

665 **FIGURE 1.** Centrifuge assay workflow.

666 **(A)** i. Ten seeds (highlighted in pink) are sown onto the surface of sterile, solid gel growth
667 medium in a single 90 mm Petri plate in two horizontal rows. ii. The plates are stacked in
668 groups of five and orientated vertically at approximately 80° to encourage the roots to grow
669 down the surface of the gel medium. Plates are grown in a growth chamber with constant light
670 (120-145 µmol m^{-2} s^{-1}) conditions at 22°C and 60% relative humidity.

671 **(B)** After 5-6 days, i. seedlings are visually analysed and numbered. ii. Petri plates are placed
672 into a swing-out-bucket centrifuge in an inverted orientation with their roots pointing inward
673 (indicated by the purple arrows). iii. After seedlings have been subjected to each one-minute
674 pulse of increasing centrifugal speed, seedling detachment is recorded.

675 **(C)** i. The aerial tissue mass of each seedling is determined using ii. an analytical scale to iii.
676 determine the root-gel adhesion properties of candidate lines are compared to wild-type to
677 assess whether they have increased (e.g. line y) or decreased (e.g. line x) adhesion to the sterile
678 gel.

679

680 **FIGURE 2** Physical root hair properties contribute to root-substrate adhesion in *Arabidopsis*
681 *thaliana.*

682 **(A)** Root hair phenotypes of 5-d-old wild-type (Col-0), *lrx 1-4, csld3-1, cow1-3, rol1-2,* and
683 *gdi1-2* seedlings grown on gel medium and statistical comparisons of mean root hair density
684 (number per mm length of root) and mean root hair length (mm) for each mutant line relative
685 to wild type. White asterisks on the root hair images indicate the characteristic root hair bulging
686 phenotype in the *lrx1-4* mutant and the short, branching root hair phenotype in *gdi1*-2. Scale
687 bar = 0.5 mm. In the table, the mean ± standard error is given for root hair density and root hair
688 length of wild type and each mutant as well as a mean comparison to wild type, which is listed
689 in bold. "No difference" is stated when there was no statistically significant difference between
690 wild type and a mutant line. The statistical output of each univariate linear model is given.
691 Alpha = 0.025, statistical significance codes: '***' = < 0.001, '**' = < 0.01. The results shown
692 are from a representative experiment for at least two independent experiments. Survival curves
693 displaying the proportion of seedlings that adhered to the gel at increasing centrifugal force for
694 **(B)** 92 wild type (Col-0 – black); 81 *lrx1-4* (light green); 70 *csld3-1* (green); **(C)** 82 wild type
695 (Col-0 - black); 83 *cow1-3* (green); and **(D)** 77 wild type (Col-0- black); 85 *rol1-2* (light green);
696 and 86 *gdi1-2* (dark green). Circled red crosses on the survival curves represent seedlings that
697 remained adhered to the gel after the maximum centrifugal speed (1611 RPM). The results

698 shown are from a representative experiment for at least two independent experiments showing
699 a statistically significant difference in adhesion between mutant lines relative to wild type (Cox
700 PH regression; alpha = 0.01). A single experiment included ≥ 70 biological replicates for each
701 candidate line.
702
703 **FIGURE 3** Vesicle trafficking mechanisms that contribute to root-substrate adhesion in
704 *Arabidopsis thaliana.*
705 **(A)** Root hair phenotypes of 5-d-old wild-type (Col-0), *syp121, syp122-1, chc1-2* and *chc2-3*
706 seedlings grown on a gel medium and statistical comparisons of mean root hair density (number
707 per mm length of root) and mean root hair length (mm) for each mutant line relative to wild
708 type. Scale bar = 0.5 mm. In the table, the mean ± standard error is given for the root hair
709 density and root hair length of wild type and each mutant as well as a mean comparison to wild
710 type, which is listed in bold. "No difference" is stated when there was no statistically significant
711 difference between wild type and a mutant line. The statistical output of each univariate linear
712 model is given. Alpha = 0.025. The results shown are from a representative experiment for at
713 least two independent experiments. Survival curves displaying the proportion of seedlings that
714 adhered to the gel at increasing centrifugal force for **(B)** 87 wild type (Col-0 – black); 91 *syp121*
715 (turquoise); 83 *syp122-1* (blue/grey); and **(C)** 83 wild type (Col-0 – black); 70 *chc1-2* (dark
716 blue); and 72 *chc2-3* (medium blue). Red crosses circled on the survival curves represent
717 seedlings that remained adhered to the gel after the maximum centrifugal speed (1611 RPM).
718 The results shown are from a representative experiment for at least two independent
719 experiments showing a statistically significant difference in adhesion between all mutant lines
720 relative to wild type (Cox PH regression; alpha = 0.01). A single experiment included ≥ 70
721 biological replicates for each candidate line.
722
723 **FIGURE 4** Exudate composition changes root-substrate adhesion properties in *Arabidopsis*
724 *thaliana.*
725 **(A)** Root hair phenotypes of 5-d-old wild-type (Col-0), *jin1-9, pdr2* and *pft1-3* seedlings grown
726 on a gel medium and statistical comparisons of mean root hair density (number per mm length
727 of root) and mean root hair length (mm) for each mutant line relative to wild type. Scale bar =
728 0.5 mm. In the table, the mean ± standard error is given for the root hair density and root hair
729 length of wild type and each mutant as well as a mean comparison to wild type, which is listed
730 in bold. "No difference" is stated when there was no statistically significant difference between
731 wild type and a mutant line. The statistical output of each univariate linear model is given.

732 Alpha = 0.025. The results shown are from a representative experiment for at least two
733 independent experiments. **(B)** Survival curves displaying the proportion of seedlings that
734 adhered to the gel at increasing centrifugal force for 80 wild type (Col-0 – black), 81 *jin1-9*
735 (light pink), 80 *pdr2* (light orange), and 81 *pft1-3* (dark orange). The results shown are from a
736 representative experiment for at least two independent experiments showing a statistically
737 significant difference in adhesion between mutant lines relative to wild type (Cox PH
738 regression; alpha = 0.01), except for *jin1-9*. A single experiment included ≥ 70 biological
739 replicates for each candidate line.
740
741 **FIGURE 5** Using the centrifuge assay in a forward genetic screen to identify *Arabidopsis*
742 *thaliana* root-substrate adhesion mutants.
743 **(A)** T-DNA insert locations in *ABCG43* for each *abcg43* mutant allele, with insertions
744 indicated by orange arrowheads. The *ABCG43* gene is located on chromosome four at position
745 Chr4: 8,969,677-8,702,727 and contains 23 exons (dark green) and 22 introns (white gaps).
746 *abcg43-1* has a T-DNA insert in the exon10/intron10 boundary, *abcg43-2* (SALK_201207)
747 has a T-DNA insert in exon 2 and *abcg43-3* (SALKseq_30713) has a T-DNA insert in exon 3.
748 **(B)** Genomic PCR confirming the homozygosity of each *abcg43* mutant for the respective T-
749 DNA inserts. Lanes **1** and **2** were loaded with the gene-specific and T-DNA-border PCR
750 products from *abcg43* mutant lines. Lanes **3** and **4** were loaded with the gene-specific and T-
751 DNA-border PCR products from a wild type (Col-0) genomic DNA template. Lanes **5** and **6**
752 were loaded with the water controls for the gene-specific and T-DNA-border PCR reactions,
753 respectively. '**L**' indicates the 100-bp ladder. The expected product sizes for the gene-specific
754 PCRs were ~350 nt, ~1025 nt and ~1090 nt; the T-DNA-border PCR product sizes were ~400
755 nt, ~550 nt and ~750 nt for *abcg43-1, abcg43-2* and *abcg43-3* alleles, respectively. **(C)**
756 Survival curves displaying the proportion of seedlings that adhered to the gel at increasing
757 centrifugal force for 79 wild type (Col-0 – black), 70 *abcg43-1* (dark pink), 85 *abcg43-2*
758 (purple), and 73 *abcg43-3* (light purple). Red crosses circled on the survival curves represent
759 seedlings that remained adhered to the gel after the maximum centrifugal speed (1611 RPM).
760 The results are from a representative experiment for at least two independent experiments
761 showing a statistically significant difference in adhesion between the mutant lines relative to
762 wild type (Cox PH regression; alpha = 0.01). A single experiment included ≥ 70 biological
763 replicates for each candidate line.

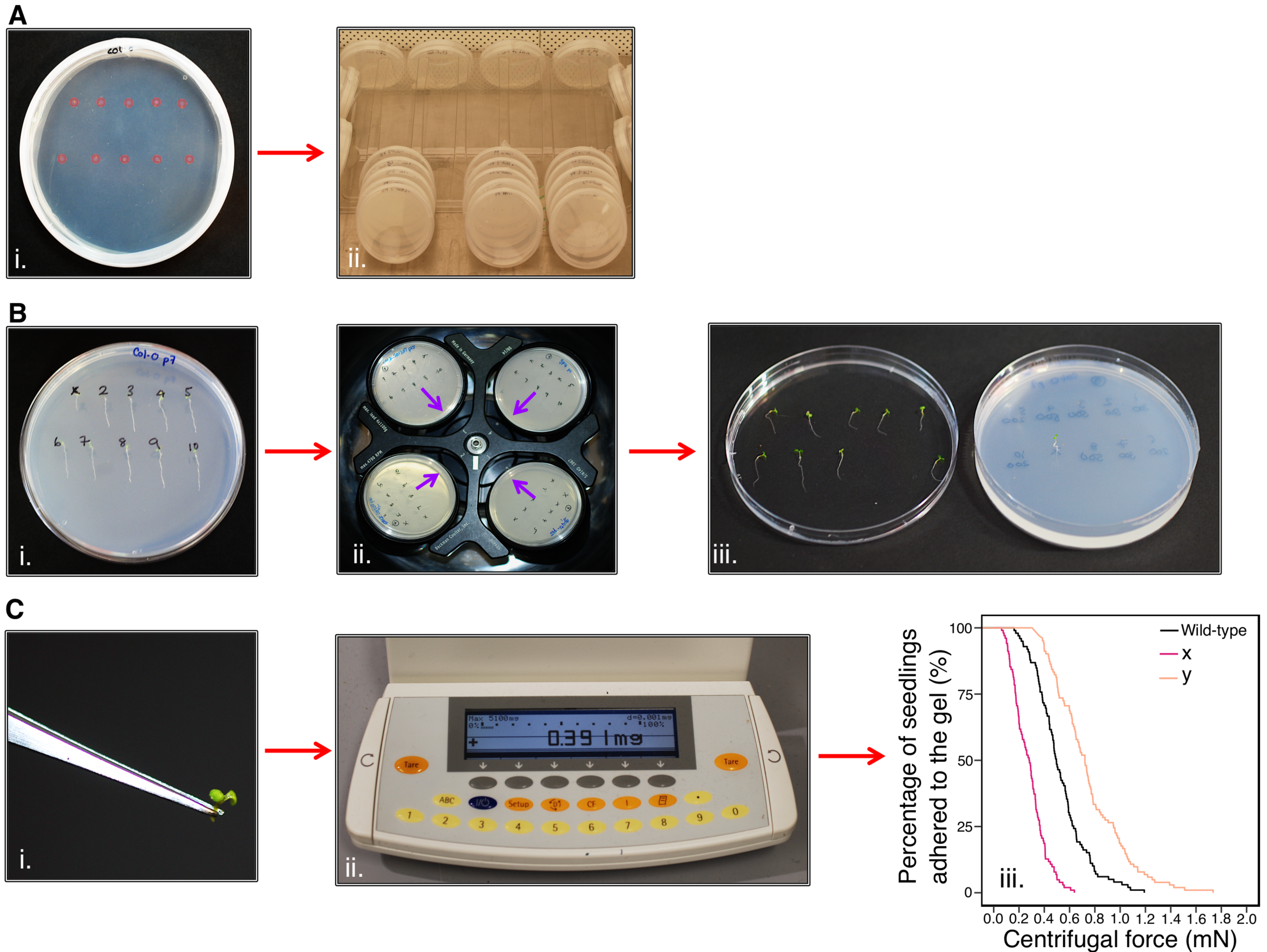
A
i.
ii.
B
Col-0 P7
x 2 3 4 5
6 7 8 9 10
i.
ii.
iii.
C
i.
ii.
Max 5100mg
d=0.001mg
0.39 1mg
Tare
Setup
CF
iii.
Percentage of seedlings adhered to the gel (%)
100
75
50
25
0
Wild-type
x
y
0.0 0.2 0.4 0.6 0.8 1.0 1.2 1.4 1.6 1.8 2.0
Centrifugal force (mN)

A

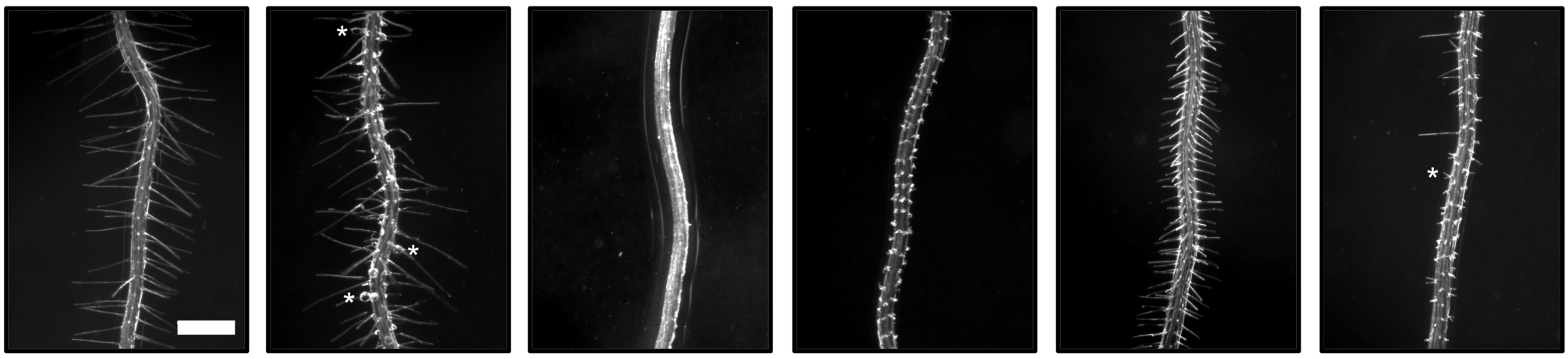

Line	Root hair density (number per mm length of root)		Root hair length (mm)	
Col-0	30.556 ± 0.784	-	0.518 ± 0.009	-
lrx1-4	31.889 ± 0.935 **No difference**	t = 1.093, P > 0.05 d.f. = 16, *n* = 9	0.388 ± 0.008 **1.3 times shorter****	t = -2.819, P < 0.001 d.f. = 16, *n* = 9
csld3-1	8.778 ± 1.188 **3.5 times less*****	t = -15.30, P < 0.001 d.f. = 16, *n* = 9	0.045 ± 0.002 **10.1 times shorter*****	t = -11.790, P < 0.001 d.f. = 16, *n* = 9
cow1-3	29.200 ± 0.772 **No difference**	t = -1.23, P > 0.05 d.f. = 17, *n* = 10	0.049 ± 0.001 **10 times shorter*****	t = -12.37, P < 0.001 d.f. = 17, *n* = 10
rol1-2	30.700 ± 1.550 **No difference**	t = 0.08, P > 0.05 d.f. = 17, *n* = 9	0.195 ± 0.003 **2.7 times shorter*****	t = -8.417, P < 0.001 d.f. = 17, *n* = 10
gdi1-2	26.200 ± 1.041 **0.17 times less****	t = -3.282, P < 0.01 d.f. = 17, *n* = 9	0.135 ± 0.006 **3.8 times shorter*****	t = -9.04, P < 0.001 d.f. = 16, *n* = 9

B

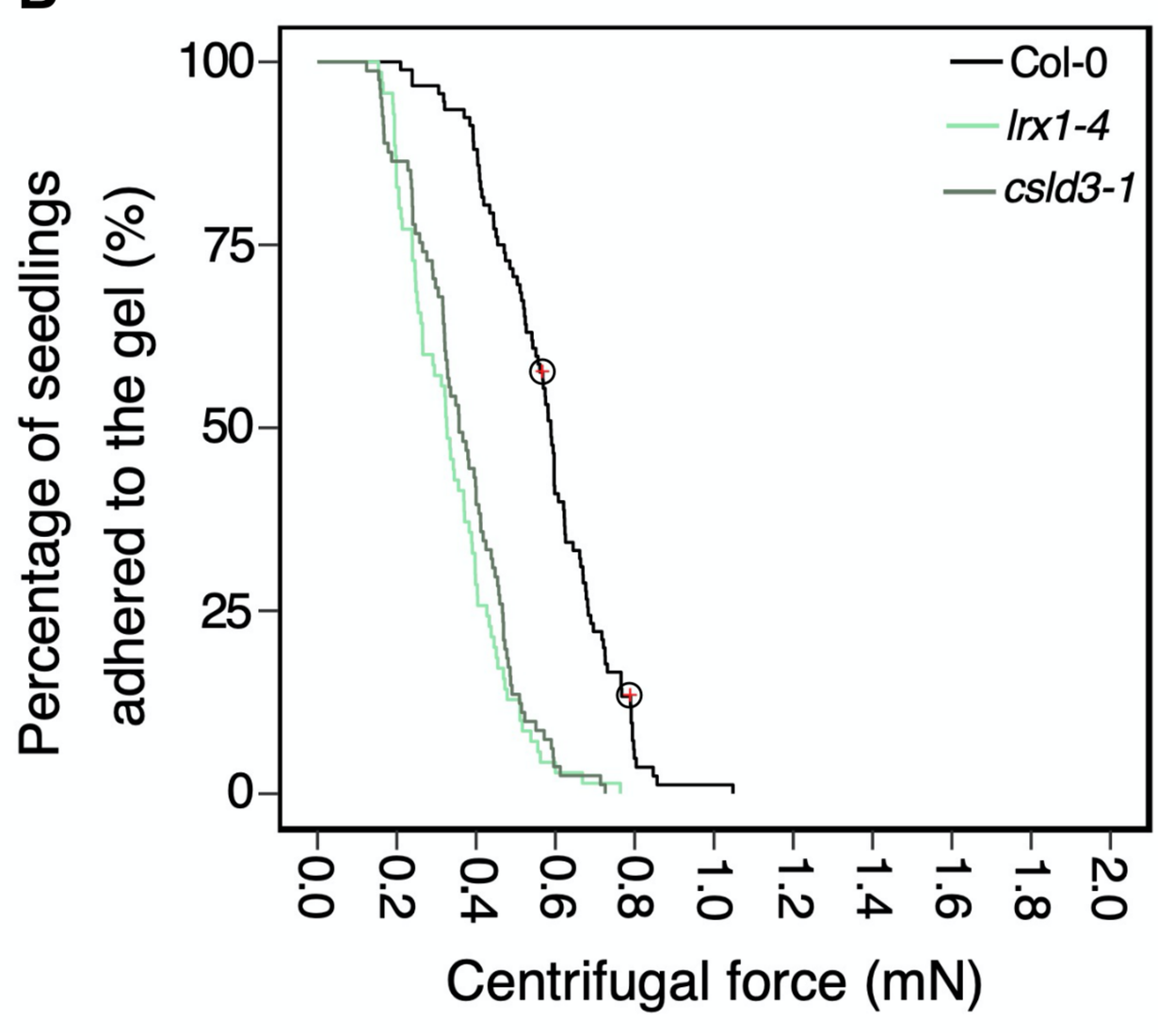

C

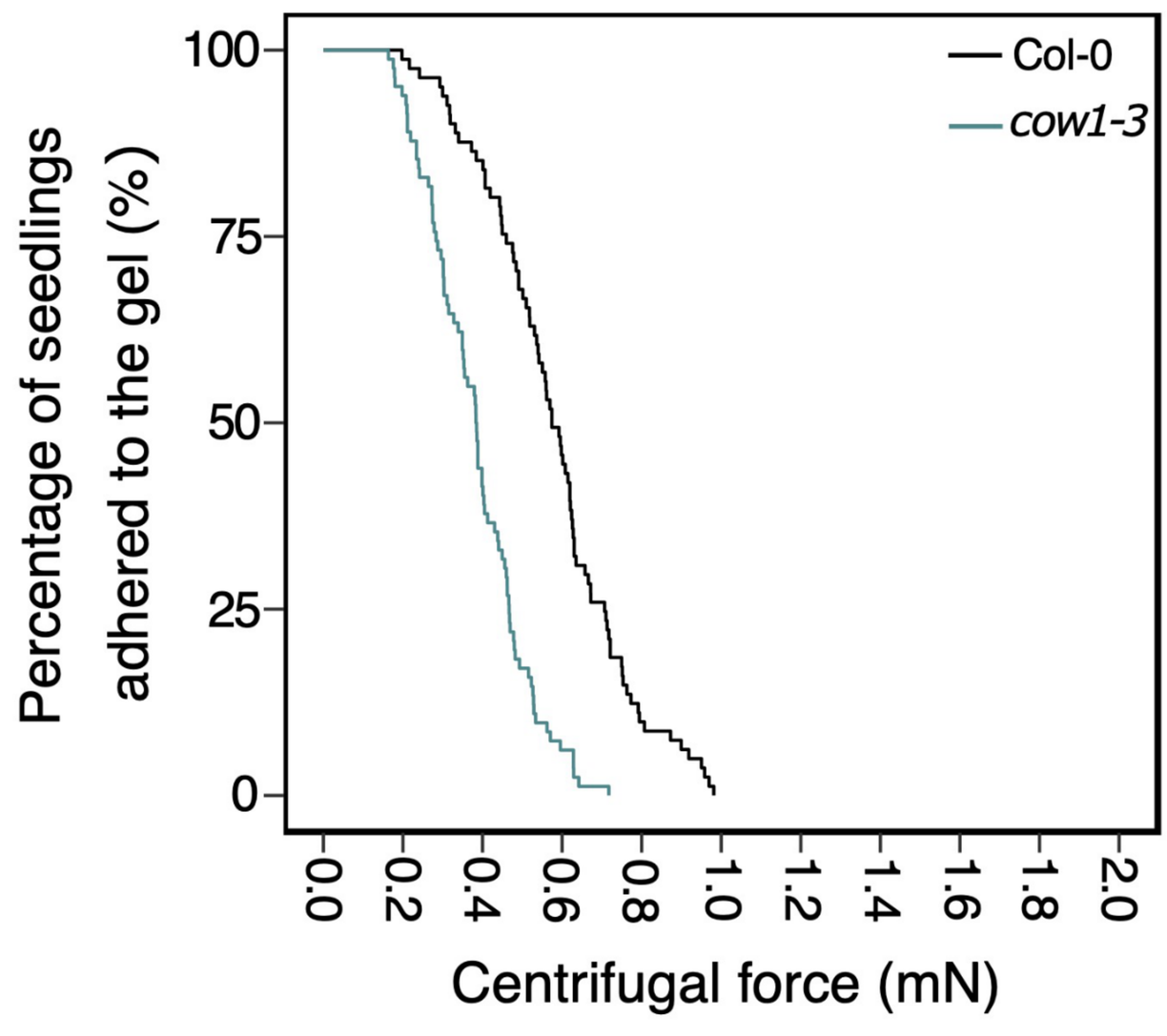

D

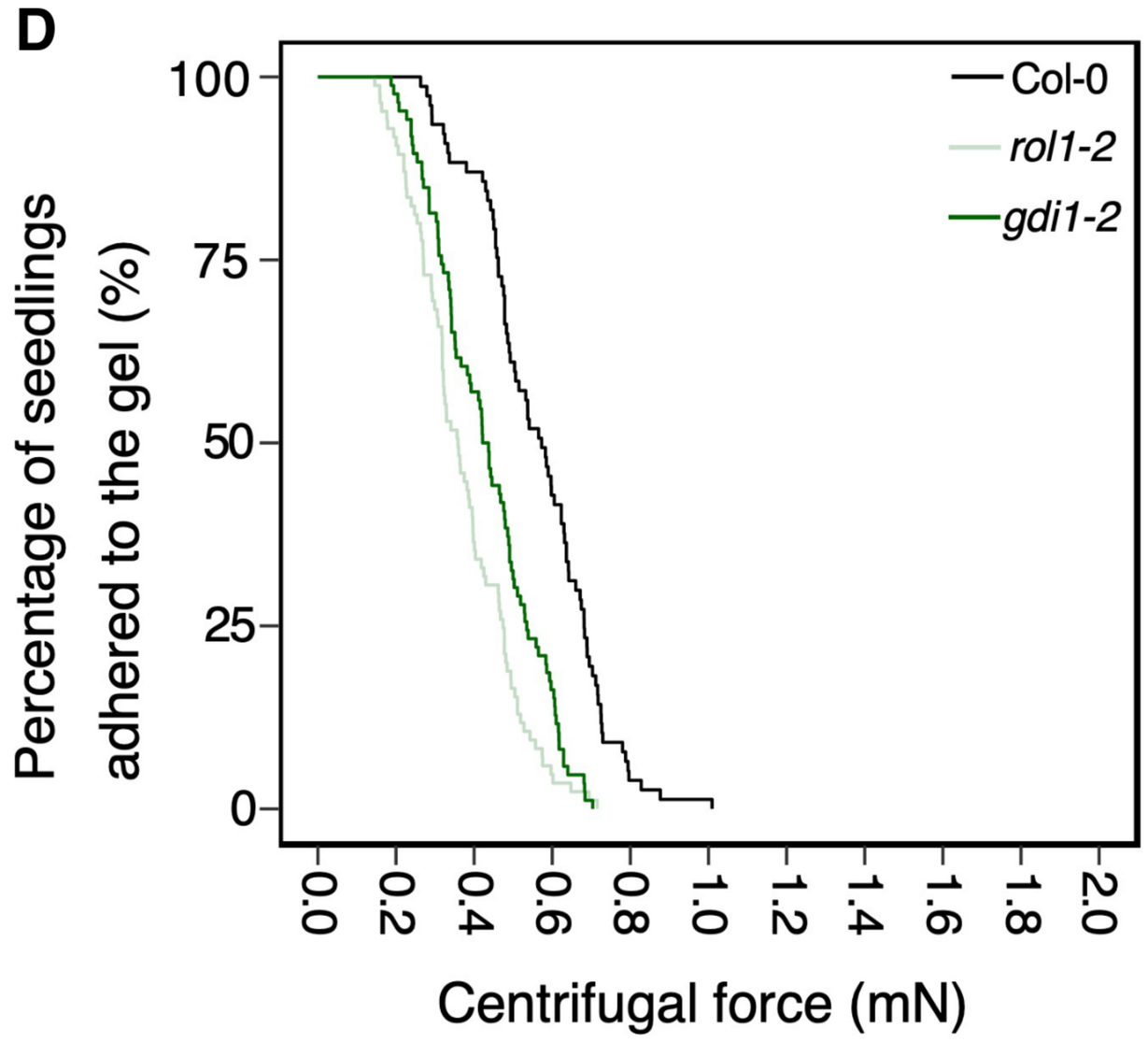

A

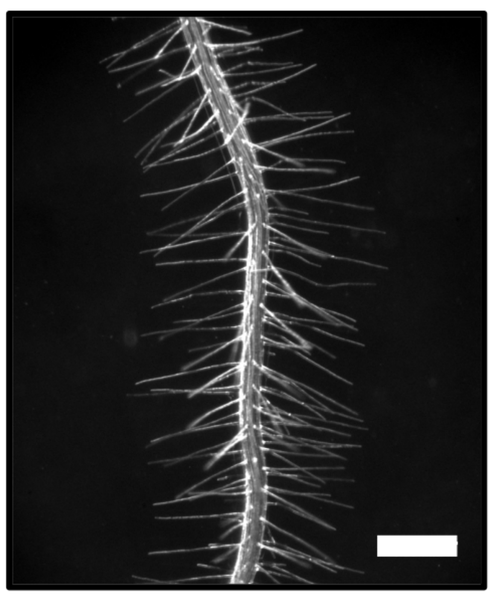

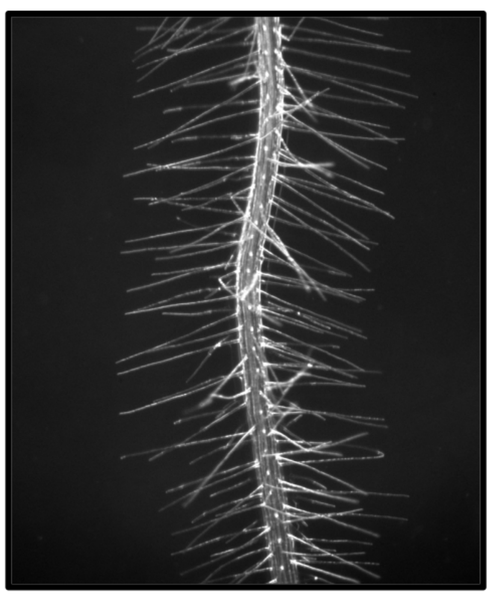

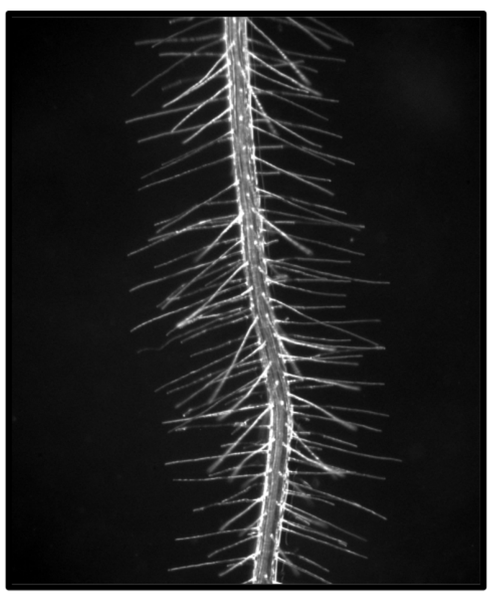

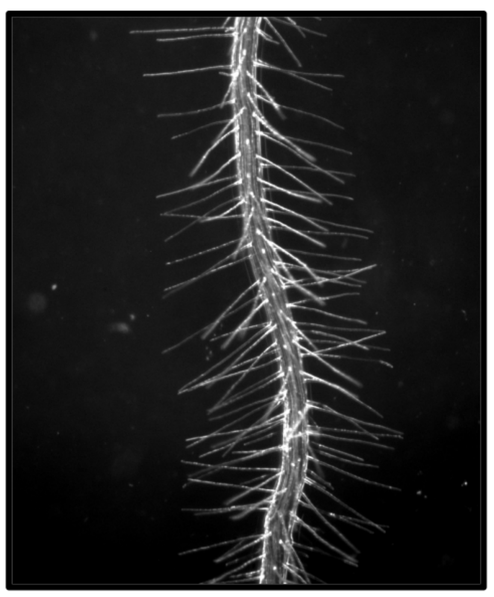

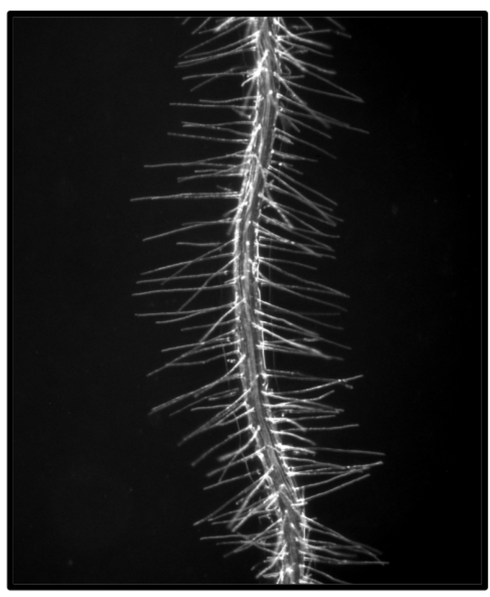

Line	***Root hair density (number per mm length of root)***		***Root hair length (mm)***	
Col-0	32.000 ± 0.632	-	0.420 ± 0.005	-
syp121	31.200 ± 0.952 **No difference**	t = -0.700, P > 0.05 d.f. = 18, *n* = 10	0.461 ± 0.004 **No difference**	t = 1.974, P > 0.05 d.f. = 18, *n* = 10
syp122-1	32.200 ± 0.442 **No difference**	t = 0.259, P > 0.05 d.f. = 18, *n* = 10	0.452 ± 0.005 **No difference**	t = 1.379, P > 0.05 d.f. = 18, *n* = 10
chc1-2	30.889 ± 0.716 **No difference**	t = -1.168, P > 0.05 d.f. = 17, *n* =9	0.441 ± 0.006 **No difference**	t = 0.684, P > 0.05 d.f. = 17, *n* = 9
chc2-3	31.889 ± 0.790 **No difference**	t = -0.111, P > 0.05 d.f. = 17, *n* = 9	0.463 ± 0.006 **No difference**	t = 0.182, P > 0.05 d.f. = 18, *n* = 10

B

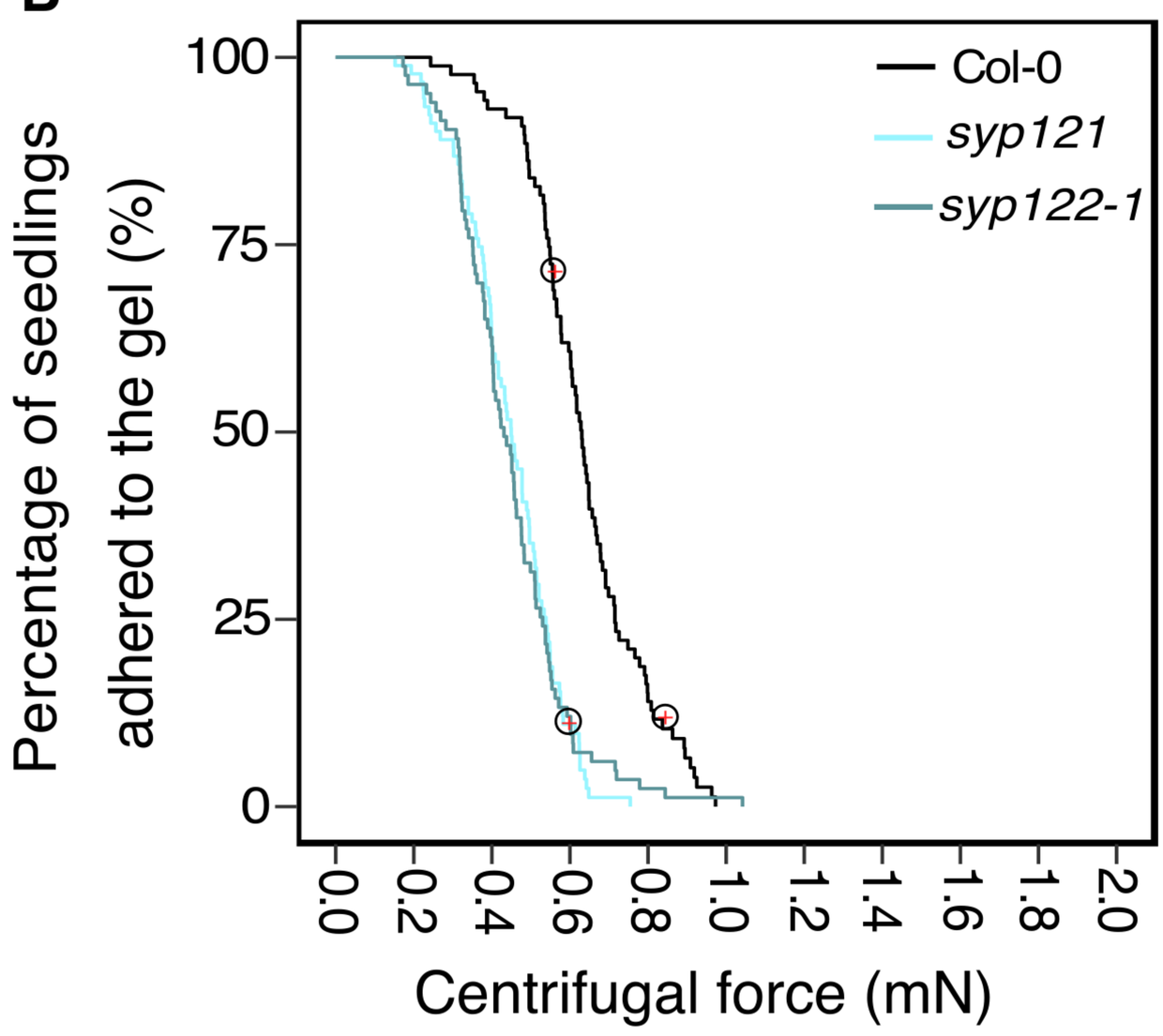

C

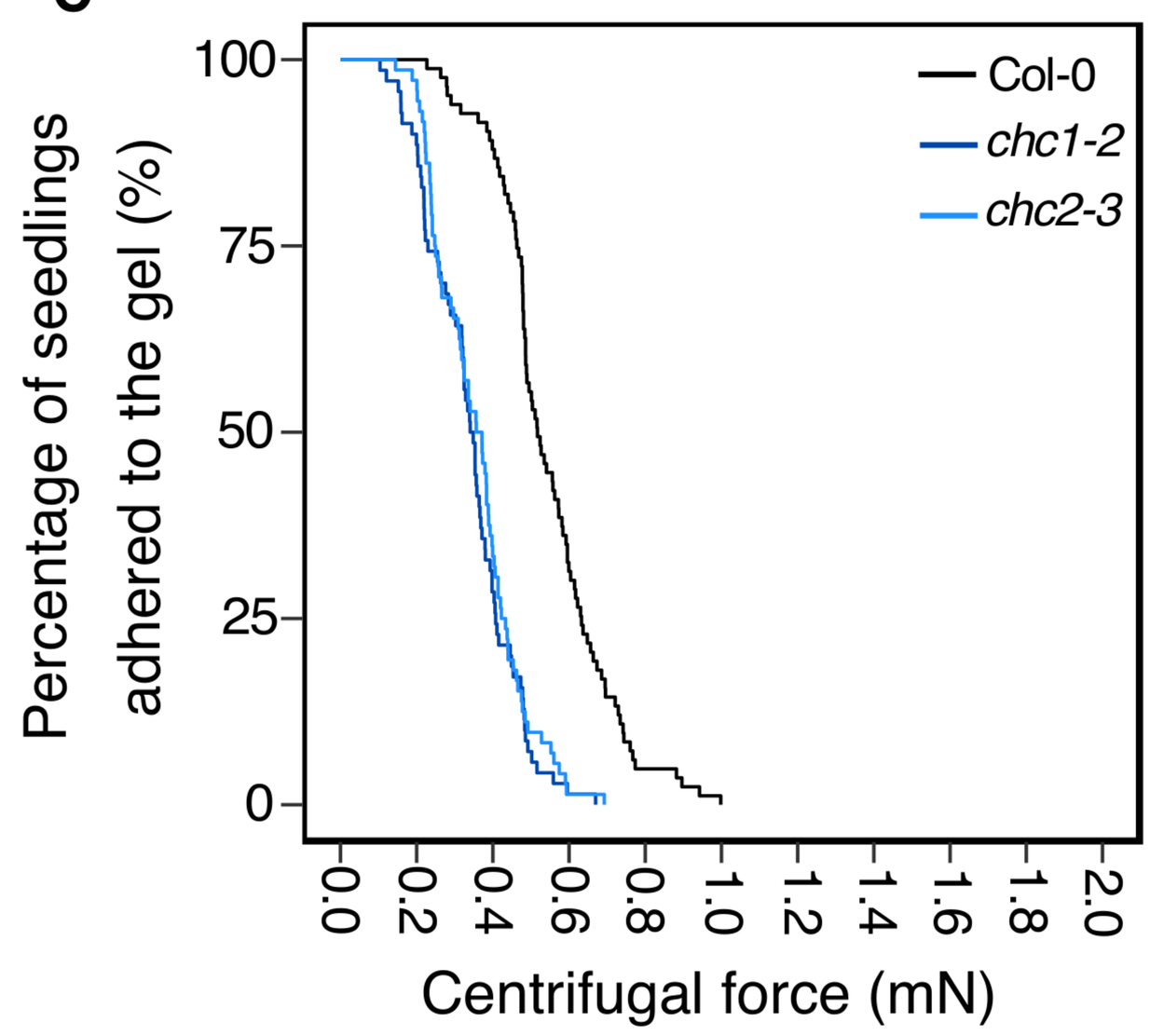

A

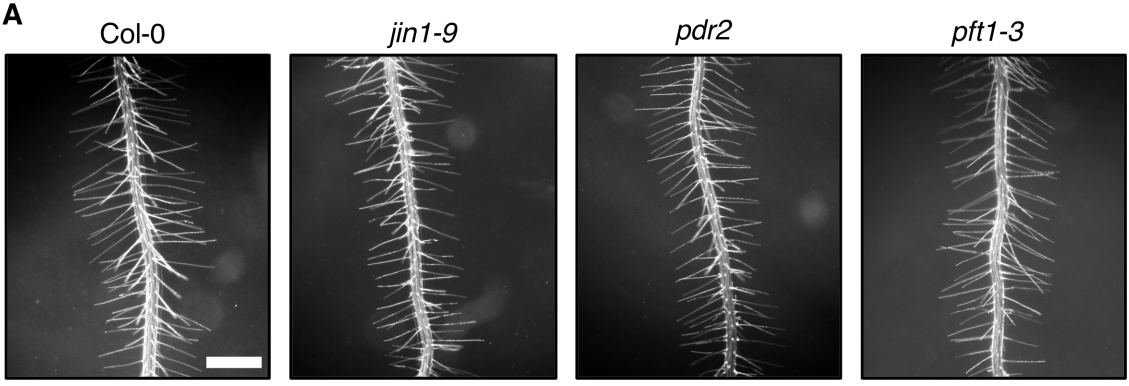

Line	*Root hair density (number per mm length of root)*		*Root hair length (mm)*	
Col-0	30.111 ± 1.612	-	0.416 ± 0.005	-
jin1-9	29.444 ± 1.271 **No difference**	t = -0.324, P > 0.05 d.f. = 16, *n* = 9	0.429 ± 0.006 **No difference**	t = 0.555, P > 0.05 d.f. = 16, *n* = 9
pdr2	31.125 ± 0.854 **No difference**	t = 0.533, P > 0.05 d.f. = 15, *n* =8	0.428 ± 0.006 **No difference**	t = 0.521, P > 0.05 d.f. = 15, *n* = 8
pft1-3	29.000 ± 1.179 **No difference**	t = -0.555, P > 0.05 d.f. = 16, *n* = 9	0.424 ± 0.006 **No difference**	t = 0.295, P > 0.05 d.f. = 16, *n* = 9

B

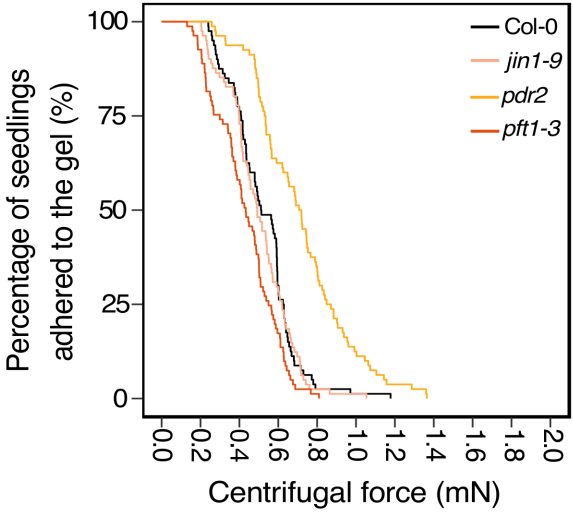

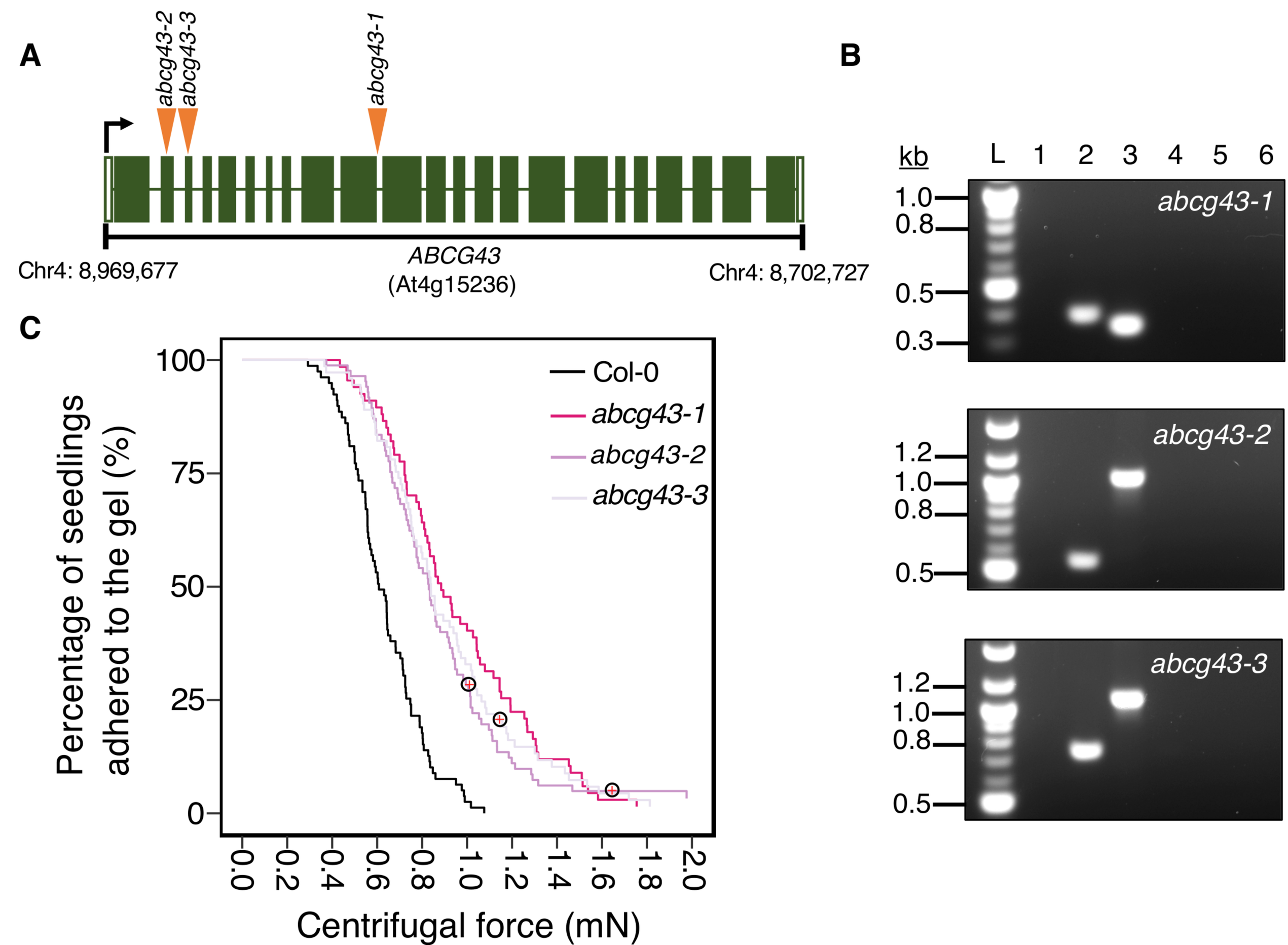
A
abcg43-2
abcg43-3
abcg43-1
Chr4: 8,969,677
ABCG43
(At4g15236)
Chr4: 8,702,727
B
kb
L 1 2 3 4 5 6
1.0
0.8
0.5
0.3
abcg43-1
1.2
1.0
0.8
0.5
abcg43-2
1.2
1.0
0.8
0.5
abcg43-3
C
Percentage of seedlings adhered to the gel (%)
100
75
50
25
0
Col-0
abcg43-1
abcg43-2
abcg43-3
0.0 0.2 0.4 0.6 0.8 1.0 1.2 1.4 1.6 1.8 2.0
Centrifugal force (mN)